# Validation of the SIRF Resolution Enhancement Algorithm for Scatterometer Data Using SAR Imagery

**Quinn P. Remund and David G. Long**
**Brigham Young University, MERS Laboratory**
**459 CB, Provo, UT 84602**
**801-378-4884, FAX: 801-378-6586**
**remundq@ee.byu.edu, long@ee.byu.edu**

*Abstract*— The inherently low resolution of spaceborne scatterometer measurements, limits the utility of this data in studies of land and ice surfaces. The scatterometer image reconstruction (SIR) algorithm was developed to increase the resolution of reconstructed scatterometer imagery by using multiple passes of the satellite. SIRF imagery created from data collected by the NASA scatterometer (NSCAT) is generated and compared to ERS-2 and RADARSAT SAR imagery. The comparisons show that SIRF images have higher resolution than nonenhanced gridded images. Low-pass filtered strips from the SAR image as well as small point targets are used to show that the effective resolution of the NSCAT imagery is on the order of 10 km.

## INTRODUCTION

Microwave scatterometry has proven an invaluable tool in many scientific disciplines. These instruments are used to estimate wind vectors over the ocean, soil-moisture content, polar sea ice extent, among many other important surface parameters. However, the nominal resolution of these instruments is typically quite low. For example, the NASA scatterometer (NSCAT) had an antenna pattern with dimensions on the order of 25 km. While the low resolution is not generally a concern for observing large scale phenomena, these values are typically too low to be useful in many land and ice studies. Synthetic aperture radar (SAR) imagery provides much better resolution measured in meters rather than kilometers. Unfortunately, these instruments usually have narrow measurement swaths and hence very low coverage of the earth's surface.

Resolution enhancement techniques such as the scatterometer image reconstruction (SIR) algorithm [1] have been developed to increase the resolution of reconstructed microwave imagery. These methods use overlapping swaths of data to increase the sampling density. SIR imagery from a variety of sensors has been successfully used in a number of studies. This paper compares SIR with filtering (SIRF) reconstructed NSCAT imagery with RADARSAT and ERS-2 SAR imagery in an effort to provide validation of the algorithm's effectiveness.

## BACKGROUND

Data collect from three spaceborne remote sensing instruments are used in this study. The first is the NASA scatterometer. NSCAT is a dual-polarization Ku-band (14 GHz) fan beam scatterometer that flew from August 1996 through June 1997. The instrument uses Doppler filtering to increase the measurement resolution and measures $\sigma^o$ at multiple incidence and azimuth angles. RADARSAT SAR is a C-band (5.3 GHz) hh-pol synthetic aperture radar. This instrument operates in a number of different modes offering several different resolutions and incidence angle ranges. Finally, the active microwave instrument (AMI) aboard the European remote sensing satellite (ERS-2) has the ability to operate in SAR mode. This SAR is a C-band (5.3 GHz) hh-pol instrument with a similar incidence angle range.

Over a limited range of incidence angles, $\theta \in [20, 55]$, Ku-band $\sigma^o$ (in dB) has a nearly linear dependence on incidence angle given by

$$10 log_{10} \sigma^\circ = A + (B - 40^\circ) \qquad (1)$$

where $A$ is $\sigma^o$ normalized to 40° and $B$ is the incidence angle dependence of $\sigma^o$. We use $A$ and $B$ coefficients to study scatterometer data processed in several ways. NSCAT $A$ and $B$ imagery are reconstructed using two different techniques for comparison with the SAR imagery. The first is nonenhanced image reconstruction in which a linear regression on NSCAT measurements is performed in 22.25 x 22.25 km grid bins which are similar in dimension to the intrinsic resolution of the NSCAT measurements. Next, the SIRF algorithm is used to generate NSCAT $A$ and $B$ images. SIRF includes damping on the nonlinear updates to reduce noise amplification. A trade-off exists between resolution and noise level. SIR applied to radiometer data was shown to be very similar in behavior to the Backus-Gilbert Inversion resolution enhancement technique [2].

## SCATTEROMETER SIRF VS. SAR COMPARISON

The comparison of active microwave imagery produced from data sets with different frequencies, polarizations, and incidence angles introduces several difficulties. Different features may be observed in the images since $\sigma^o$ is a function of all three of these parameters. However, comparison of the images reveals that similar features can be

0-7803-5207-6/99/$10.00 

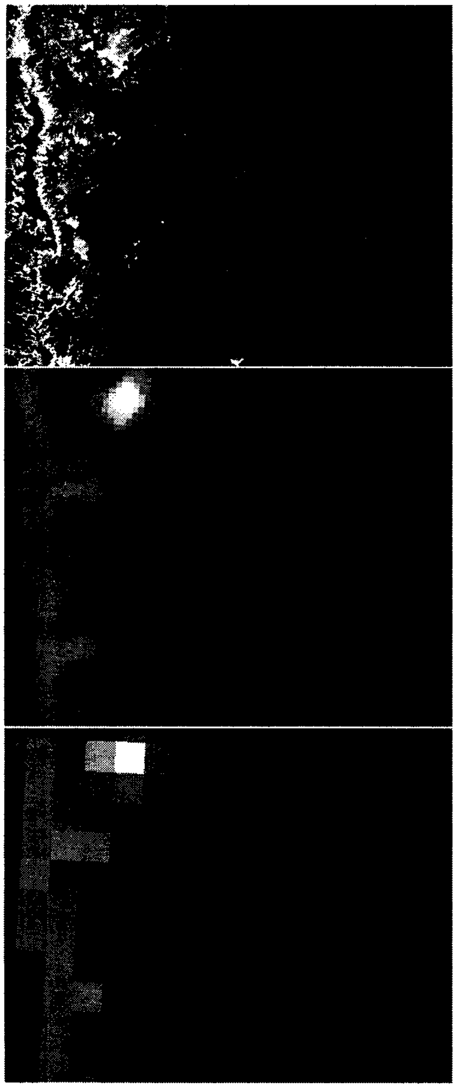

**Figure 1**: Image resolution comparison. From top to bottom, RADARSAT SAR (400m), NSCAT $A_v$ SIRF, NSCAT $A_v$ NON.

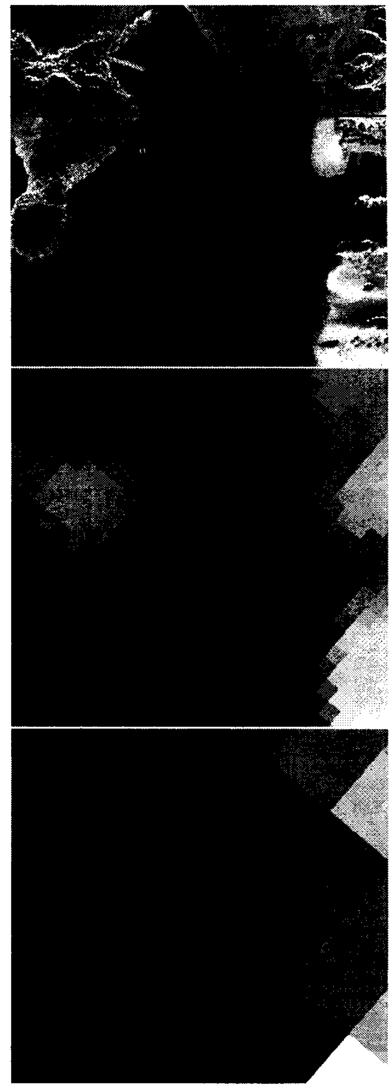

**Figure 2**: Image resolution comparison. From top to bottom, ERS-2 SAR (100m), NSCAT $A_v$ SIRF, NSCAT $A_v$ NON.

found in each. To ease the comparison, the images are normalized. While it is not possible to completely remove the differences, the images are standardized so that each image has pixels values with zero mean and unit variance.

NSCAT v-pol $A$ images ($A_v$) are created using six days of data for comparison with the SAR imagery. A qualitative comparison of reconstructed images with SAR images is found in Figures 1-2. Figure 1 is a comparison of reconstructed images with a RADARSAT SAR frame from orbit 05994 frame number 733. The image covers a 334 x 270 km area with 400 meter pixel spacing. A portion of the Antarctic Peninsula visible on the left side of the image with sea ice to the right. The same basic features are observed in all of the images. On the left side, glacial ice with characteristically high $\sigma^o$ is present. The dark band in the middle is likely a mixture of young ice and open water. The medium scale values to the right are older forms of ice with greater surface roughness. SIRF shows much greater detail than the nonenhanced image. In particular, a large nearly elliptical ice floe is observed in the middle of the SAR image. This is also evident in the SIRF image. The same feature is much more difficult to discern in the nonenhanced image.

Figure 2 illustrates a comparison of ERS-2 SAR orbit

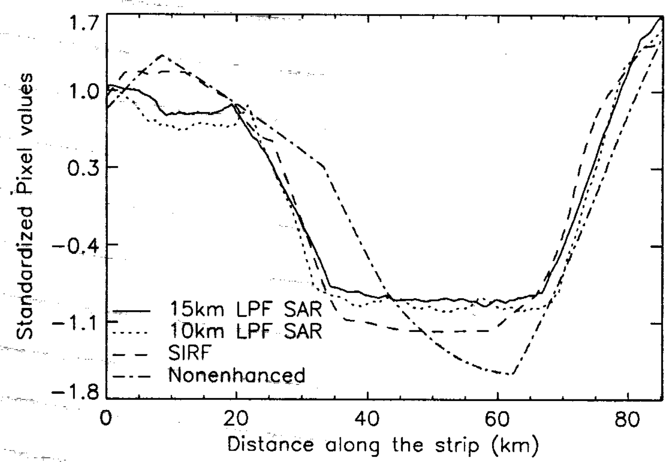


**Figure 3**: Comparison of standardized pixel values along a horizontal strip of an ERS-2 SAR frame.

07353 frame 660 with NSCAT $A_v$ images. These images cover a 100 x 97 km region containing the volcanic Ross Island (upper left) as well as portions of the Ross Ice Shelf (top edge and right side). McMurdo station is near the upper edge of the image slightly to the left of center. Again the same trend is observed. Compared to the nonenhanced image, SIRF has the best feature definition, particularly for the ice shelf and island edges. The nonenhanced image is the poorest with only a few pixels in the entire region.

We now consider the resolution characteristics along a horizontal strip of pixels in the ERS-2 SAR frame from Figure 2. The location of the strip is shown as a horizontal black line in the image. Since the SIRF and nonenhanced images both have far less pixel values along the slice, bilinear interpolation is implemented to interpolate the values between pixel centers. The SAR strip is then convolved with increasingly large uniform blurring functions. Figure 3 shows a plot of pixel values in the strip from all three images. The SAR image has been convolved with both a 10 and 15 km wide blurring function. The plot again verifies that SIRF is more highly correlated with the SAR image than the nonenhanced reconstruction. We also note that the SIRF image strip values generally follow the 10 km filtered SAR curve better than 15 km version. In particular, the slopes match up well for SIRF and the 10 km filtered SAR in the transition regions.

The last resolution comparison uses a small, bright feature at the bottom middle of the SAR image in Figure 1. This feature has a width of approximately 3 km which is smaller than the SIRF pixel dimensions and consequently can be treated as a point target in the reconstruction. We note that the NSCAT SIRF image also exhibits this feature and is approximately 2 pixels wide. This strengthens the previous argument that the NSCAT SIRF resolution is on the order of 10 km at least for stationary targets.

## CONCLUSION

The scatterometer image reconstruction with filter (SIRF) algorithm can be used to increase the resolution of scatterometer imagery. Comparisons with SAR imagery show that SIRF generated NSCAT imagery have significantly higher resolution than nonenhanced gridded images. Based on an examination of point targets and low-pass filtered SAR strips, we conclude that the NSCAT SIRF resolution is on the order of 10 km. Further evaluation is continuing.

## ACKNOWLEDGMENTS

NSCAT data provided by the PO.DAAC at the Jet Propulsion Laboratory. ERS-2 and RADARSAT SAR data obtained from the Alaskan SAR facility.

## REFERENCES

[1] D. Long, P. Hardin, and P. Whiting, "Resolution Enhancement of Spaceborne Scatterometer Data," *IEEE Trans. on Geosci. and Rem. Sens.*, vol. 31, pp. 700–715, 1993.

[2] D.G. Long and D.L. Daum, "Spatial Enhancement of SSM/I Data," *IEEE Trans. Geosci. Remote Sens.*, vol. 36, pp. 407–417, 1997.